



Injection Locking of a Trapped-Ion Phonon Laser

S. Knünz,¹ M. Herrmann,¹ V. Batteiger,¹ G. Saathoff,¹ T. W. Hänsch,¹ K. Vahala,² and Th. Udem¹

¹Max-Planck-Institut für Quantenoptik, 85748 Garching, Germany

²California Institute of Technology, Pasadena, California 91125, USA

(Received 17 February 2010; published 2 July 2010)

We report on injection locking of optically excited mechanical oscillations of a single, trapped ion. The injection locking dynamics are studied by analyzing the oscillator spectrum with a spatially selective Fourier transform technique and the oscillator phase with stroboscopic imaging. In both cases we find excellent agreement with theory inside and outside the locking range. We attain injection locking with forces as low as $5(1) \times 10^{-24}$ N so this system appears promising for the detection of ultraweak oscillating forces.

DOI: 10.1103/PhysRevLett.105.013004

PACS numbers: 37.10.Vz, 05.45.Xt, 07.10.Pz, 37.10.Ty

By injecting a weak harmonic signal, a stronger self-sustained oscillator at sufficiently close frequency can be forced to phase synchronize with the injected signal. Since its first description by Huygens in pendulum clocks [1], injection locking (or entrainment) has found widespread applications. It was observed in a variety of systems, as diverse as organ pipes [2], solid state oscillators [3], optomechanical radio frequency (rf) oscillators [4], and optical lasers [5]. In this Letter we report injection locking of an almost ultimately simple and well-controlled system, the motion of a single, harmonically bound ion.

A Mg^+ ion, held in a linear rf trap, is addressed by two laser beams tuned below (red detuned) and above (blue detuned) an atomic resonance, respectively. While the red-detuned laser damps the motion of the ion, the blue-detuned laser provides gain by amplifying an existing motion. For appropriate settings of laser detunings and intensities, regenerative oscillations with a stable amplitude start from noise. The forces due to the laser beams saturate as periodic Doppler shifts are induced by the ion motion. Recently, we could show that the amplification is due to the stimulated generation of vibrational quanta (phonons) and that the system represents a mechanical analogue of an optical laser, a phonon laser [6].

We study the action of a weak, harmonic rf signal tuned close to the motional resonance on the dynamics of this oscillator using two different techniques, which both rely on the good spatial and temporal resolution of our imaging system. With the first method, a spatially selective Fourier transform technique, we obtain the motional spectrum of the oscillator. The second method, stroboscopic imaging, allows us to retrieve the phase of the ion relative to the drive. All our observations agree very well with theory, further substantiate the analogy to an optical laser, and extend its applicability. Our analysis reveals that we attain injection locking with minute forces as small as $5(1)$ yN (yocto $\equiv 10^{-24}$). This great sensitivity might allow the detection of nuclear spin flips of single atomic or molecular ions.

Injection locking is a well-understood phenomenon [7,8]. Let us review some basic features for later reference: consider an oscillator of free-running frequency ω_0 , mass m , and linewidth γ . A weak oscillation induced by an injected auxiliary rf signal of frequency ω_i and voltage U_i is amplified by the blue-detuned laser. The gain of this auxiliary frequency component is proportional to [7]

$$|g(\delta)|^2 \approx \frac{\gamma^2}{\delta^2} \quad (1)$$

for sufficiently large detunings $\delta = \omega_i - \omega_0$. As the detuning decreases, the injected signal takes up more of the limited gain available from the blue-detuned laser. The gain at the free oscillation reduces accordingly; once it drops below threshold only the oscillation at ω_i prevails—the oscillator is injection locked to the external source [7]. Assuming the injected signal is weak, the total oscillation amplitude of the regenerative oscillator stays approximately unchanged in this process and we focus our discussion on their relative phase.

The relative phase $\phi(t)$ in the transient and steady-state regime is described by the Adler equation [8],

$$\frac{d\phi(t)}{dt} + \delta = -\omega_m \sin\phi(t), \quad (2)$$

where ω_m denotes half the locking range. In terms of experimentally accessible parameters, we find for our system

$$\omega_m = \frac{eE_i}{2m\omega_0 x_0}. \quad (3)$$

Here, E_i denotes the electric field due to the injected signal U_i at the position of the ion and x_0 the oscillation amplitude. A solution of Eq. (2) inside the locking range yields a fixed relative phase and reads

$$\phi(\delta) = \sin^{-1}\left(-\frac{\delta}{\omega_m}\right). \quad (4)$$

The phase lag varies between $+\pi/2$ and $-\pi/2$ as δ is tuned from $-\omega_m$ to $+\omega_m$ and changes sign at $\delta = 0$.

Solving Eq. (2) outside the locking range ($|\delta| > \omega_m$) yields a time-dependent phase of the oscillator [7]

$$\tan \frac{\phi(t)}{2} = -\frac{\omega_b}{\delta} \tan \frac{\omega_b(t - t_0)}{2} - \frac{\omega_m}{\delta}. \quad (5)$$

Here t_0 incorporates the initial conditions and the time-averaged phase advance $|\langle d\phi/dt \rangle| = \omega_b = \sqrt{\delta^2 - \omega_m^2}$. This causes the oscillator frequency ω to be pulled towards the injected frequency ω_i

$$\omega = \omega_i - \text{sgn}(\delta)\omega_b \approx \omega_0 + \frac{\omega_m^2}{2\delta}, \quad (6)$$

where the approximation holds for large detunings.

Figure 1 shows the experimental setup (see also [6,9]). A $^{24}\text{Mg}^+$ ion is stored in a linear rf ion trap which consists of four symmetrically arranged tungsten rods, each 80 mm long and 2 mm in diameter. The distance from the trap center to each electrode surface is 1.475 mm. The trap is driven at 22.6 MHz and a rf amplitude that leads to a radial secular oscillation frequency of ≈ 700 kHz. We study injection locking of the ion's axial motion; in this direction confinement is provided by a dc voltage U_{dc} applied to two metal rings of 12.5 mm diameter and separated by 18.5 mm. We typically work with $U_{\text{dc}} \approx 400$ V; thus, $\omega_0 \approx 2\pi \times 50$ kHz. The injected signal is generated with a rf synthesizer (ω_i, U_i) connected to a third ring electrode (8 mm diameter, 35 mm from the trap center). By measuring the displacement of an ion for several (high) dc voltages applied to this electrode, we find that a voltage of 1 V exerts a force of 50(1) yN, which corresponds to an electric field of about 0.3 mV/m. The ion is observed with

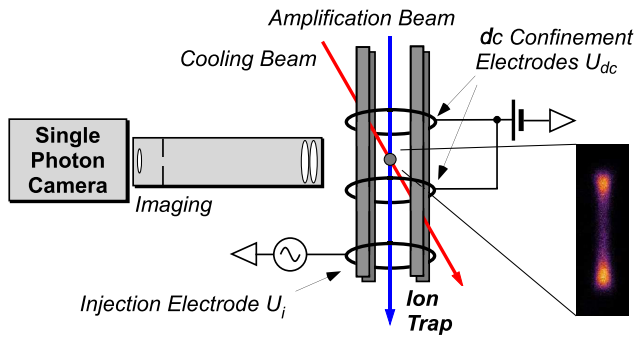


FIG. 1 (color online). Experimental setup. Two laser beams address a single ion in a linear Paul trap located in a vacuum chamber. Axial confinement is generated by a dc voltage applied to two ring-shaped electrodes. The injected signal is introduced by a signal generator connected to a third ring electrode. A single-photon camera detects the ion fluorescence. The magnified inset shows as an example a time-averaged image of the optically driven ion oscillation. Since the ion spends more time at the turning points of the oscillation they appear brighter, which results in a characteristic double-lobed pattern.

a $f/2$, $2 \mu\text{m}$ resolution imaging system attached to a single-photon camera (Quantar Mepsicron II) with a timing jitter below 100 ps. We excite regenerative oscillations of the Mg^+ ion by driving the $3s_{1/2} - 3p_{3/2}$ transition near 280 nm (natural linewidth 42 MHz) [10] with two laser beams. Both beams are referenced to a frequency comb [11] and set to detunings $\Delta_{c,g}$ and intensities $I_{c,g}$. Typically, those are $\Delta_c = -70$ MHz for the cooling laser and $\Delta_g = +10$ MHz for the gain laser, the cooling laser intensity is about one tenth of the saturation intensity. With the gain laser intensity set to zero, the ion is Doppler cooled to a temperature of ≈ 1 mK and has an observed FWHM of $\approx 5 \mu\text{m}$, limited by the thermal spread of the ion in the trapping potential and the resolution of our optics. At an intensity ratio of $I_g/I_c \approx 0.2$, we observe stable oscillations with an amplitude of $\approx 30 \mu\text{m}$. The time-averaged ion images show a characteristic double-lobed pattern (inset of Fig. 1), indicating a coherent oscillation [6]. The parameters given above vary slightly from experiment to experiment in order to optimize the measurement conditions.

In order to directly measure the motional frequency spectrum, we implemented a spatially selective Fourier transform scheme [Fig. 2(a)]. Here, we electronically select only fluorescence photons that originate from one of the turning points of the motion. Since the ion appears periodically in this region, the photon count rate is modulated by the motional frequency. The camera encodes the position of each detected photon in two voltages. Four electronic comparator units select a rectangular region of the image within which the photon trigger signal is forwarded and analyzed by a spectrum analyzer. Note that this scheme also allows one to measure the motional spectrum of any oscillating ion within a chain or crystal of ions.

To study the influence of the injected signal we set its amplitude to $U_i = 5$ V and record spectra for several detunings. Figure 3 shows three characteristic examples. In Fig. 3(a) the injected signal is far outside the locking range. The width of the (Lorentzian) free-running component implies a quality factor of 1400. Additionally, a mo-

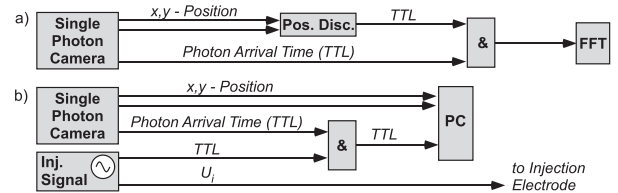


FIG. 2. Single-photon camera signal processing schemes. (a) The position resolving detection electronics to select the photons emitted within only one part of the double-lobed pattern to directly extract the ion's motional spectrum (pos. disc.: position discriminator; TTL: transistor transistor logic type signal; FFT: spectrum analyzer). (b) Stroboscopic imaging by electronically selecting photons that were detected within a certain phase window relative to the injected signal.

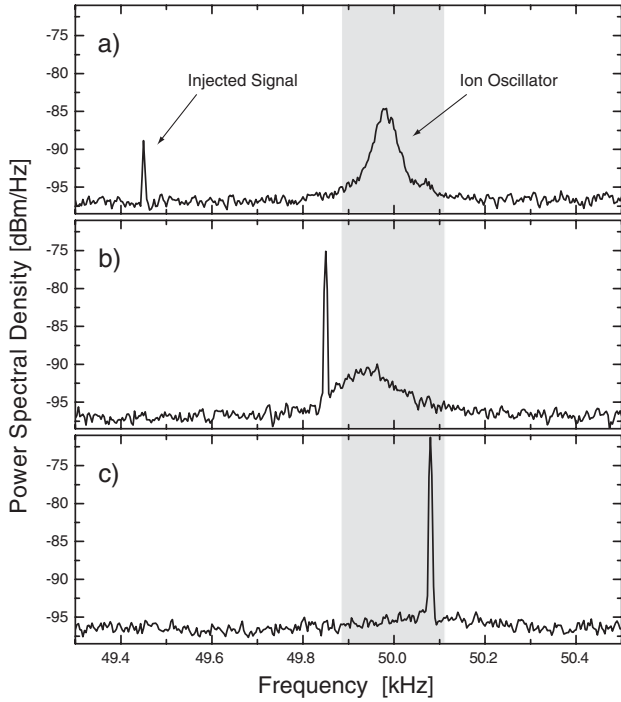


FIG. 3. Measured motional frequency spectra [Fig. 2(a)] of a single ion inside and outside the locking range (shaded area). In (a) and (b) both the ion oscillation and the injected frequency are visible. The spectral width of the ion oscillation is due to damping and spontaneous emission; the width of the injected signal is limited by the instrumental resolution. In (b) the injected signal was set closer to the unperturbed frequency of the ion. As expected, the injected signal is amplified at the expense of the free-running oscillation. Further, the free-running frequency is pulled towards the injected signal and its width has increased. Within the locking range (c), only the amplified injected signal prevails.

tional component at the frequency of the injected signal is visible as a small, resolution limited (5 Hz) peak. In Fig. 3(b) the injected signal approaches the locking range and the spectrum shows three interesting features. First, the frequency of the free-running component is pulled towards the injected frequency [Eq. (6)]. Second, the amplitude of the free-running component decreases as the injected signal is amplified [Eq. (1)]. Third, the linewidth increases, so the quality factor drops to 400. This is similar to the Schawlow-Townes limit of an optical laser which is inversely proportional to the power [12]. In Fig. 3(c), the ion oscillator is injection locked and only one resolution limited component is left. Figure 4 shows a quantitative analysis of frequency pulling which is in good agreement with theory.

In a second set of measurements we studied the phase of the ion oscillation relative to the injected frequency using stroboscopic imaging. Here we accept only photons that arrive within a certain phase window relative to the injected signal. This is implemented by exploiting the excellent

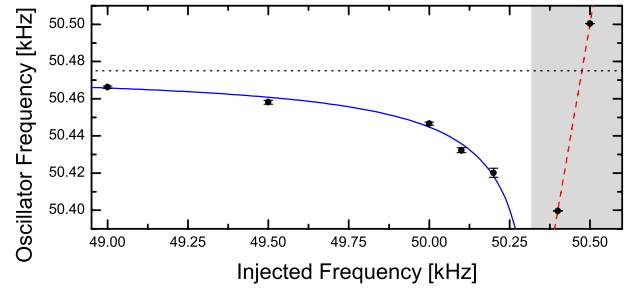


FIG. 4 (color online). Frequency pulling. The measured ion oscillation frequency $\omega/2\pi$ is plotted versus $\omega_i/2\pi$. The shaded area marks the locking range, the dashed red line is a plot of $\omega = \omega_i$, while the horizontal dotted line marks the free-running frequency $\omega_0/2\pi$. The solid blue line is a fit of the exact part of Eq. (6) to the data points outside the locking range.

timing resolution of our single-photon camera [Fig. 2(b)]. We use logic operations to define a phase window of $\approx 13^\circ$ for the acceptance of photons. In the images acquired this way, the double-lobed pattern collapses to a spot within the locking range, the position of which allows one to retrieve the phase $\phi(\delta)$. With x denoting the position of the ion, more precisely the center of gravity of the image, and x_0 the oscillation amplitude, the relative phase angle can be determined within the locking range by $\sin^{-1}(x/x_0)$.

We acquire stroboscopic images for 200 frequency data points centered around ω_0 in random order. Each image is exposed for 2 s, so it represents an average over $\sim 10^5$ oscillation cycles. In a next step we project the two-dimensional images onto the oscillation axis and calculate the center of gravity of this distribution (Fig. 5). The locking range is marked by the two extrema. Inside the locking range the ion has a fixed phase relation to the injected signal [Eq. (4)] and the double-lobed pattern collapses to a spot [Figs. 5(a) and 5(c)]. Outside the locking range a double-lobed pattern is observed; however, it is asymmetric since the phase is modulated according to Eq. (5). This asymmetry increases as the injected frequency approaches the locking range. Intuitively, this is because the power of the free-running oscillation diminishes in favor of the injected signal (Fig. 3). A fit to the data [Eqs. (2), (4), and (5)] that includes an unintentional phase delay in our electronics of $\approx 12.1^\circ$ and the finite phase window of $\approx 13^\circ$ delivers remarkable agreement. The phase delay is responsible for the slight asymmetry visible in Fig. 5. The rather steep slope of the dispersion shaped behavior inside the locking range implies high sensitivity to frequency changes of the oscillator which might be interesting for mass spectrometry [13].

Following the same procedure sketched above, the locking range was determined for several excitation voltages U_i , secular frequencies ω_0 , and oscillation amplitudes x_0 . In all cases we find good agreement with the predictions by Eq. (3).

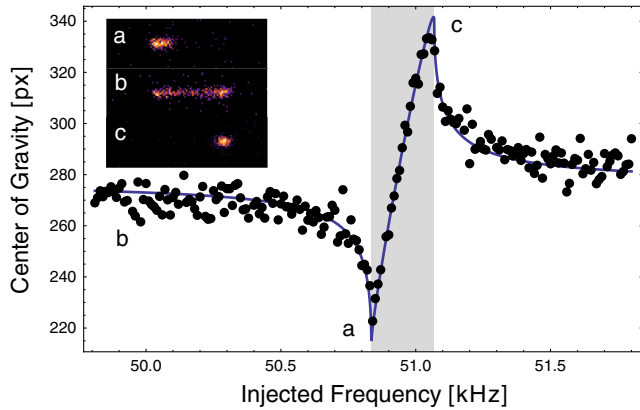


FIG. 5 (color online). Stroboscopic imaging [Fig. 2(b)]. Plot of the center of gravity of the ion image in pixels (px) versus the injected frequency. The injection locking range is marked by the shaded area which coincides with the two phase extrema. Inside, the oscillator has a fixed phase relation to the injected signal and the center of gravity follows Eq. (4). Outside the locking range we observe a phase pull-in behavior, Eq. (5). The solid line is a fit which includes a constant phase delay introduced by our electronics that leads to the visible slight asymmetry. The inset shows exemplary phase sensitive stroboscopic ion images: (b) outside the locking range, the double-lobed pattern is visible; (a) and (c) inside the locking range. Here the ion oscillator has a fixed phase relative to the injected signal and thus collapsed to a spot.

We were able to observe injection locking with voltages as low as 100 mV, which corresponds to a force of only $5(1)$ yN acting on the ion. The tininess of this force is due to the low mass of an ion compared to, e.g., a cantilever of an atomic force microscope [14], and the great sensitivity of the presented techniques. To set a scale, note that for our trapping parameters a force of 5 yN displaces an ion by only about 1 nm, which is 2% of the spread of the ion's wave function if it was cooled to the motional ground state, while our ion was only Doppler cooled to 1 mK (thermal spread ~ 4000 nm). The use of trapped ions as force probes has recently been considered theoretically for the case of ground-state cooled ions in [15]; an experiment based on Doppler velocimetry that was able to detect 174 yN is reported in [16]. The sensitivity of our system seems to be limited by phase noise due to spontaneous emission and technical instabilities and is the subject of further investigations.

Compared to established force detectors, the ion appears as a rather unusual atomic-scale force probe. How could it be utilized for a measurement? Consider, for example, the detection of the nuclear magnetic moment of a single atomic or molecular ion trapped together with an auxiliary ion. A magnetic field gradient dB/dr , generated, e.g., by a

small current loop or a tiny ferromagnetic tip, induces a force $F = g\mu_N m_I dB/dr$, where g is the Landé factor, μ_N the nuclear magneton, and m_I the nuclear spin. For feasible gradients of several 100 T/m, this results in a force of roughly 10 yN. If a microwave or rf field then induces spin flips at a Rabi frequency close to a motional frequency of the ion pair, the resulting oscillating force can injection lock a motional mode. We already demonstrated a force sensitivity of 5 yN, so such an experiment seems feasible in principle. This would allow one to study nuclear magnetic resonance signals in molecules unperturbed by a solvent for the first time. Moreover, measurements would be possible even if the hyperfine structure is not accessible by current laser technology.

In conclusion, we have demonstrated injection locking of a trapped-ion phonon laser. Our observations are all in excellent agreement with theory and deepen the analogy of our system to optical lasers. Further, we demonstrated the detection of oscillating forces as weak as $5(1)$ yN, using a straightforward experimental setup involving ions merely cooled to the Doppler limit. The presented techniques could be applied to measure the nuclear magnetic moment of single atoms or molecules.

We gratefully acknowledge T. Wilken for the frequency comb and M. Hori for helpful discussions. This research was supported by the DFG cluster of excellence "Munich Center for Advanced Photonics." K. V. gratefully acknowledges support from the Alexander von Humboldt foundation and also thanks Caltech. T.W.H. acknowledges support by the Max-Planck Foundation.

-
- [1] M. Bennett *et al.*, *Proc. R. Soc. A* **458**, 563 (2002).
 - [2] M. Abel *et al.*, *Phys. Rev. Lett.* **103**, 114301 (2009).
 - [3] K. Kurokawa, *Proc. IEEE* **61**, 1386 (1973).
 - [4] M. Hossein-Zadeh and K.J. Vahala, *Appl. Phys. Lett.* **93**, 191115 (2008).
 - [5] H.L. Stover and W.H. Steier, *Appl. Phys. Lett.* **8**, 91 (1966).
 - [6] K.J. Vahala *et al.*, *Nature Phys.* **5**, 682 (2009).
 - [7] A.E. Siegman, *Lasers* (University Science Books, Sausalito, CA, 1986).
 - [8] R. Adler, *Proc. IRE* **34**, 351 (1946).
 - [9] V. Batteiger *et al.*, *Phys. Rev. A* **80**, 022503 (2009).
 - [10] M. Herrmann *et al.*, *Phys. Rev. Lett.* **102**, 013006 (2009).
 - [11] B. Bernhardt *et al.*, *Opt. Express* **17**, 16 849 (2009).
 - [12] A. Yariv, *Quantum Electronics* (John Wiley & Sons, New York, 1989), p. 581.
 - [13] M. Drewsen *et al.*, *Phys. Rev. Lett.* **93**, 243201 (2004).
 - [14] H.J. Mamin and D. Rugar, *Appl. Phys. Lett.* **79**, 3358 (2001).
 - [15] R. Maiwald *et al.*, *Nature Phys.* **5**, 551 (2009).
 - [16] M. Biercuk *et al.*, arXiv:1004.0780v3.